REPORT DOCUMENTATION PAGE			Form Approved OMB No. 0704-0188

1. AGENCY USE ONLY (*Leave blank*)	2. REPORT DATE	3. REPORT TYPE AND DATES COVERED

4. TITLE AND SUBTITLE
QUADRUPLET EXPANSION OF THE ACOUSTIC PRESSURE FIELD IN A WEDGE SHAPED OCEAN

5. FUNDING NUMBERS

6. AUTHOR(S)
JOYCE, MICHAEL D.

7. PERFORMING ORGANIZATION NAME(S) AND ADDRESS(ES)
NAVAL POSTGRADUATE SCHOOL
MONTEREY, CA 93943-5000

8. PERFORMING ORGANIZATION REPORT NUMBER

9. SPONSORING/MONITORING AGENCY NAME(S) AND ADDRESS(ES)

10. SPONSORING/MONITORING AGENCY REPORT NUMBER

11. SUPPLEMENTARY NOTES
THE VIEWS EXPRESSED IN THIS THESIS ARE THOSE OF THE AUTHOR, AND DO NOT REFLECT THE OFFICIAL POLICY OR POSITION OF THE DEPARTMENT OF DEFENSE OR THE US GOVERNMENT

12a. DISTRIBUTION/AVAILABILITY STATEMENT
Approved for public release; distribution is unlimited.

12b. DISTRIBUTION CODE

13. ABSTRACT (*Maximum 200 words*) In a wedge shaped ocean, the method of images is used to develop an analytical approximation of the acoustic pressure field. Contemporary work develops acoustic doublets from a combination of the source and surface reflection image using simple dipole theory. The method of images is then used to sum the dipole images. This thesis matches dipole pairs to achieve a quadruplet expansion. A computer program using the derived quadruplet equation is then created to verify the results by comparing them with the "URTEXT" program.

14. SUBJECT TERMS	15. NUMBER OF PAGES
METHOD OF IMAGES QUADRUPLET EXPANSION	40
	16. PRICE CODE

17. SECURITY CLASSIFICATION OF REPORT	18. SECURITY CLASSIFICATION OF THIS PAGE	19. SECURITY CLASSIFICATION OF ABSTRACT	20. LIMITATION OF ABSTRACT
UNCLASSIFIED	UNCLASSIFIED	UNCLASSIFIED	UNLIMITED

Approved for public release; distribution is unlimited.

Quadruplet Expansion of the Acoustic Pressure Field in a Wedge Shaped Ocean

by

Michael D. Joyce
Lieutenant , United States Navy
B.S., California State Polytechnic University, Pomona

Submitted in partial fulfillment
of the requirements for the degree of

MASTER OF SCIENCE IN APPLIED PHYSICS

from the

NAVAL POSTGRADUATE SCHOOL
September,1993

ABSTRACT

In a wedge shaped ocean, the method of images is used to develop an analytical approximation of the acoustic pressure field. Contemporary work develops acoustic doublets from a combination of the source and surface reflection image using simple dipole theory. The method of images is then used to sum the dipole images. This thesis matches dipole pairs to achieve a quadruplet expansion. A computer program using the derived quadruplet equation is then created to verify the results by comparing them with the "URTEXT" program.

TABLE OF CONTENTS

I. INTRODUCTION

This thesis is a continuation in the examination of the acoustic pressure field in a wedge shaped ocean. As the focus of naval operations shifts to the littoral regions, more attention is being paid to the problem of A.S.W. in acoustically shallow water, i.e. regions where the sound paths have multiple interactions with the surface and bottom. To date, the simplest propagation model has been the method of images.

In its present form, this model assumes isospeed water, a pressure release upper surface, and a lossy, penetrable bottom. For parallel surfaces, the source and its images form a vertical array with the actual source at the center. Furthermore, if the source is near the surface it can be combined with its negative (180^0 out of phase) surface reflection image to form a dipole source. The column of images can then be considered a column of doublet images.

The equations used in this thesis are the far field approximations of the acoustic doublet. An unbalanced doublet is defined as having two sources of nearly equal amplitude but opposite phase separated by a distance d. If the amplitudes differ greatly, or if the phase difference is not 180^0; then the doublet approximation is not valid.

When the method of images is used in a wedge shaped ocean, the vertical column of doublet images becomes a circle

centered on the apex. In previous work the upper and lower image doublets were summed individually with great success. This thesis attempts to group upper and lower doublets into double doublets or quadruplets.

This method can only be used for extremely small wedge angles. With larger angles the sound paths from the upper and lower doublet images will be to dissimilar, and the quadruplet approximation will be invalid. Since typical slopes for most of the worlds continental shelves are about 3^0, a good analogy would be that of using a ship mounted active sonar searching for a diesel submarine in the shelf region.

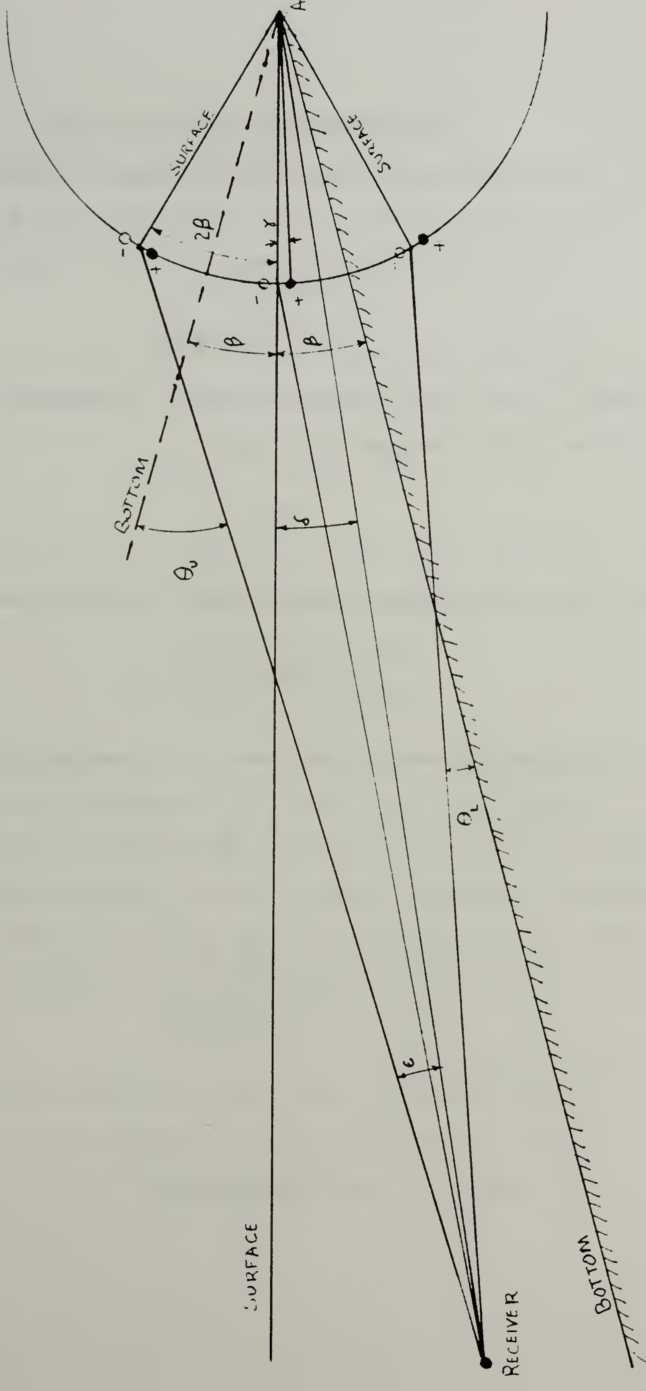

FIG. 1

II. WAVE NUMBERS AND SCALING

Sound propagation in a shallow channel with a pressure release surface parallel to a rigid bottom has a propagation wave number for each mode defined by the following equation

$$K_n = (n - \frac{1}{2}) \frac{\pi}{H} \frac{1}{f(\theta)} \tag{1}$$

Where H is the depth of the channel. For a fast bottom, θ is the critical angle found from

$$\sin\theta_c = \frac{C_1}{C_2} \tag{2}$$

An analogous reference angle θ_s for a slow bottom is

$$\tan\theta_s = \frac{C_2}{C_1} \tag{3}$$

If the depth H is replaced by the scaling distance,

$$R_s = \frac{R}{X} \tag{4}$$

and the bottom is tilted at angle β; then eq.1 for the cutoff value of the lowest mode with a fast bottom becomes

$$Kx = \frac{\pi}{2\sin\theta\tan\beta} \tag{5}$$

and for a slow bottom

$$Kx = \frac{\pi}{2\tan\theta\tan\beta} \tag{6}$$

III. ACOUSTIC DOUBLET FORMATION

The sound propagation for spherical spreading of a point source is

$$P=\frac{A_o}{r}e^{j(\omega t-kr)} \quad (7)$$

When two point sources of opposite phase are combined to form a doublet, equation 7 can be expanded,

$$P=\frac{A_+}{r_-}e^{j(\omega t-kr_-)}-\frac{A_-}{r_+}e^{j(\omega t-kr_+)} \qquad (8)$$

Where the "+" and "-" subscripts refer to the upper and lower sources respectively. These values can be expanded

$$\begin{array}{ll} r_+=r+\Delta r & A_+=A_o+\Delta A \\ r_-=r-\Delta r & A_-=A_o-\Delta A \end{array} \qquad (9)$$

Where the delta values indicate the incremental difference for each source compared to a theoretical point source located exactly between them. The pressure equation can then be rearranged to yield

$$P=\frac{A_o}{r}e^{j(\omega t-kr)}\left[\left(\frac{1+\frac{\Delta A}{A_o}}{1-\frac{\Delta r}{r}}\right)e^{jk\Delta r}-\left(\frac{1-\frac{\Delta A}{A_o}}{1+\frac{\Delta r}{r}}\right)e^{-jk\Delta r}\right] \qquad (10)$$

An acoustic source located near the surface has a surface reflection image of equal amplitude and opposite phase. In the far field the image pair is treated as a

single doublet source. For a balanced source, the pressure equation can be approximated by

$$P=\frac{A}{r}e^{j\omega t}\left[e^{-jk(r-\Delta r)}-e^{-jk(r+\Delta r)}\right] \tag{11}$$

As seen in fig. 2, Δr is

$$\Delta r=\frac{d}{2}\sin\theta \tag{12}$$

or

$$\Delta r=r_1\sin\gamma\sin\theta \tag{13}$$

combining eqs. 11 and 13, yields the pressure

$$P=2j\frac{A}{r}\sin(kr_1\sin\gamma\sin\theta)\,e^{j(\omega t-kr)} \tag{14}$$

To develop an equation for the unbalanced doublet, the amplitude relationships expressed in eq. 9 must be rewritten as

$$A_o=\frac{A_+ + A_-}{2} \qquad \Delta A=\frac{A_+ - A_-}{2} \tag{15}$$

So that for an unbalanced doublet

$$P=2\frac{jA_o}{r}\left[\sin(kr_1\sin\theta)-j\Delta\frac{A}{A_o}\cos(kr_1\sin\theta)\right]e^{j(\omega t-kr)} \tag{16}$$

The distance from the center of the doublet to the receiver can be calculated using the law of cosines.

$$r^2 = r_1^2 + r_2^2 - 2r_1 r_2 \cos(2n\beta \pm \delta) \qquad (17)$$

Where the ranges r_1 and r_2 are measured from the apex to the source, and from the apex to the receiver respectively. The angle δ is measured from the surface down to the receiver. The range from each successive doublet in a wedge of angle β is

$$r_n = \sqrt{r_1^2 + r_2^2 - 2r_1 r_2 \cos(2n\beta \pm \delta)} \qquad (18)$$

Where the angle in the cosine term refers to the angle of each reflected image; those with a "+" are the upper images, and those with a "-" are the lower images. This equation can be rearranged to yield

$$r_n = (r_1 - r_2)\sqrt{1 + \frac{2r_1 r_2}{r_1 - r_2{}^2}(1 - \cos(2n\beta \pm \delta)} \qquad (19)$$

The first order Taylor's series expansion can then be used to simplify eq. 19

$$r_n = (r_1 - r_2)\{1 + \frac{r_1 r_2}{r_1 - r_2{}^2}[1 - \cos(2n\beta \pm \delta)]\} \qquad (20)$$

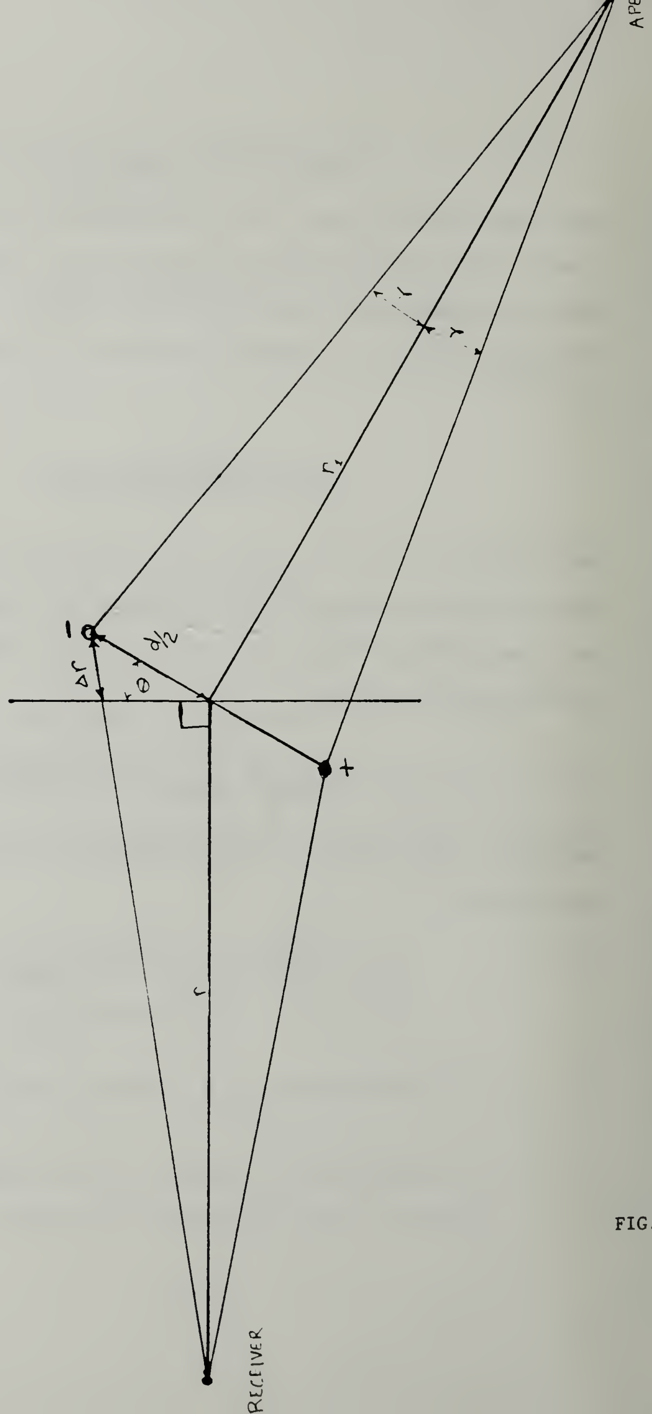

FIG. 2

IV. QUADRUPLET EXPANSION

The upper and lower image doublets can be combined to form a quadruplet. The complimentary doublets are 180^0 out of phase, and the pressure of the new quadruplet is

$$p_n = \frac{2jA_n}{r}\{\sin[kr_1\gamma\sin(2n\beta+\delta)]\,e^{-jk\Delta r_+} - \sin[kr_1\gamma\sin(2n\beta-\delta)]\,e^{-jk\Delta r_-}\}e^{j(\omega t-kr)} \tag{21}$$

In this case, both of the interior exponents involving Δr are negative. The Δr terms are derived from a comparison to the range from the primary doublet, thereby ensuring that all phase angles are calculated with respect to a common reference point. To find the Δr values used in eq. 21, an approximation of eq. 20 gives

$$\Delta r_-^+ = r_-^+ - (r_2 - r_1) = \frac{r_1 r_2}{r_2 - r_1}\,[1-\cos(2n\beta\pm\delta)] \tag{22}$$

The cosine term can be expanded and approximated for small values of δ.

$$\cos(2n\beta\pm\delta) \approx \cos(2n\beta) \pm \delta\sin(2n\beta) \tag{23}$$

Equation 21 can now be expanded into the unbalanced quadruplet equation.

$$p_n = \frac{2jA_n}{r}e^{j(\omega t-kr)}e^{-jk\frac{r_1 r_2}{r_2-r_1}(1-\cos(2n\beta))} \{\sin[kr_1\gamma\sin(2n\beta+\delta)]\,e^{-jk\frac{r_1r_2}{r_2-r_1}\delta\sin(2n\beta)} - \sin[kr_1\gamma\sin(2n\beta-\delta)]\,e^{jk\frac{r_1r_2}{r_2-r_1}\delta\sin(2n\beta)}\} \tag{24}$$

It is convenient to define

$$
\begin{aligned}
\phi &= kr_1\mu\,(1-\cos(2n\beta)) \\
d &= kr_1\delta\sin(2n\beta) \\
\mu &= \frac{r_2}{r_2-r_1}
\end{aligned}
\tag{25}
$$

So that eq. 24 becomes

$$
\begin{aligned}
p_n = \frac{2j}{r_d}\, e^{j(\omega t-kr)}\, e^{-j\phi} \\
\{A_n[\sin[kr_1\gamma\sin(2n\beta+\delta)] - j\frac{\Delta A}{A}\cos[kr_1\gamma\sin(2n\beta+\delta)]]\,e^{-j\mu d} \\
-B_n[\sin[kr_1\gamma\sin(2n\beta-\delta)] - j\frac{\Delta B}{B}\cos[kr_1\gamma\sin(2n\beta-\delta)]]\,e^{j\mu d}\}
\end{aligned}
\tag{26}
$$

The values for ΔA and ΔB must be determined from the reflection coefficients.

V. REFLECTION COEFFICIENTS FOR A SLOW BOTTOM

The reflection coefficients used in this thesis are derived from the Rayleigh reflection coefficient

$$R=\frac{bc-\sin\theta_t/\sin\theta_i}{bc+\sin\theta_t/\sin\theta_i} \qquad (27)$$

Where

$$b=\frac{\rho_2}{\rho_1} \qquad c=\frac{c_2}{c_1} \qquad (28)$$

The angles are the grazing angle θ_i and angle of transmission θ_t. Therefore, θ_c is defined as

$$\frac{c_1}{c_2}=\arccos\theta_c \qquad (29)$$

Using trigonometric relationships, eq. 27 can be rewritten.

$$R=\frac{bc-\sqrt{1-c^2\cos^2\theta_i}/\sin\theta_i}{bc+\sqrt{1-c^2\cos^2\theta_i}/\sin\theta_i} \qquad (30)$$

In addition, the term under the radical can be rewritten.

$$\sqrt{1-c^2\cos^2\theta_i}=c\sqrt{\sin^2\theta_i-\sin^2\theta_c} \qquad (31)$$

Combining eqs. 30 and 31, and rearranging yields

$$R=\frac{b-\sqrt{1-[\sin\theta_c/\sin\theta_i]^2}}{b+\sqrt{1-[\sin\theta_c/\sin\theta_i]^2}}=\frac{b-\sqrt{1-1/x^2}}{b+\sqrt{1-1/x^2}} \qquad (32)$$

Where x is

$$x=\frac{\sin\theta_i}{\sin\theta_c} \tag{33}$$

For a slow bottom with a very small angle, eq. 32 can be approximated by

$$R=e^{\frac{2bc}{\sqrt{1-c^2}}\theta_i} \tag{34}$$

The argument of the exponential is

$$\alpha=\frac{2bc}{\sqrt{1-c^2}}=\frac{2\rho_2/\rho_1}{\sqrt{(c_2/c_1)^2-1}} \tag{35}$$

So that this approximation of the Rayleigh reflection coefficient can be written in a more concise form

$$R=e^{\alpha\theta_i} \tag{36}$$

Since each ray intersects the bottom and surface multiple times, a product of reflection coefficients along each individual path is required. This cumulative coefficient will take the form

$$\mathfrak{R}_n=\prod_{m=1,3,\ldots}^{2n-1} R[\theta_i-(2n-m)\beta] \tag{37}$$

and the product yields

$$\mathfrak{R}_n=e^{n\alpha\theta_i}e^{-n^2\alpha\beta} \tag{38}$$

For very small angles, this can be approximated by

$$\Re_n = e^{-n^2 \alpha\beta} \tag{39}$$

The angles of incidence are needed to calculate the product. The angles for the bottom images are

$$\theta_o = 2(n-1)\beta \tag{40}$$

Using the law of sines, the angle at the receiver is defined

$$\epsilon = (r_1/r_0)\sin(2n\beta+\delta) \tag{41}$$

The angle of incidence of the ray from the center of the doublet image to the receiver intersecting the apparent bottom is

$$\theta = 2(n-1)\beta+\delta+\epsilon \tag{42}$$

However, the upper and lower images in each doublet have slightly different angles of incidence with the apparent bottom

$$\theta_\pm = (2n-1)\beta+\delta+\epsilon_\pm \tag{43}$$

The upper and lower angles at the receiver for each doublet are

$$\epsilon_\pm = \epsilon \pm (r_1/r_o)\gamma\cos(2n\beta+\delta) \tag{44}$$

The individual angles of incidence are

$$\theta_\pm = \theta_o + \delta(1+(r_1/r_o)\cos(2n\beta+\delta)) \pm (r_1/r_o)\gamma\cos(2n\beta) \tag{45}$$

If the following variables are used in the coefficients as approximations of the sine of the angles of incidence

$$a_n = 1 + \frac{r_1}{r_o} cos2n\beta$$
$$b_n = \frac{r_1}{r_o} cos2n\beta \qquad (46)$$

then eq. 38 becomes

$$\mathfrak{R}_{n_\pm} = \mathfrak{R}_n e^{-n\delta a_n \alpha} e^{\mp n\gamma b_n \alpha} \qquad (47)$$

For each doublet image there is an upper and lower image. The upper doublet is defined by A_n with the upper image A_- and the lower image A_+. Likewise, the lower doublet B_n has the upper image B_- and the lower image B_+.

$$A_- = \mathfrak{R}_n e^{na_n\delta\alpha} e^{nb_n\gamma\alpha} \qquad B_- = \mathfrak{R}_n e^{na_n\delta\alpha} e^{nb_n\gamma\alpha}$$
$$A_+ = \mathfrak{R}_n e^{-na_n\delta\alpha} e^{nb_n\gamma\alpha} \qquad B_+ = \mathfrak{R}_n e^{na_n\delta\alpha} e^{-nb_n\gamma\alpha} \qquad (48)$$

A_n and ΔA defined by eq. 15 can be combined with eq. 48

$$A_n = \mathfrak{R}_n \cosh(nb_n\gamma\alpha) e^{na_n\delta\alpha} \qquad B_n = \mathfrak{R}_n \cosh(nb_n\gamma\alpha) e^{na_n\delta\alpha}$$
$$\Delta A = \mathfrak{R}_n \sinh(nb_n\gamma\alpha) e^{-na_n\delta\alpha} \qquad \Delta B = \mathfrak{R}_n \sinh(nb_n\gamma\alpha) e^{na_n\delta\alpha} \qquad (49)$$

When combined, they yield

$$\frac{\Delta A}{A_n} = \tanh(nb_n\gamma\alpha) \qquad \frac{\Delta B}{B_n} = \tanh(nb_n\gamma\alpha) \qquad (50)$$

The result is the full quadruplet equation

$$P = p_1 + \sum_{n=1}^{N} \frac{2j}{r} \mathfrak{R}_n coshb\ e^{j(\omega t - kr)} e^{-j\phi}$$
$$[e^{-a-j\mu d} \sin(kr_1\gamma \sin(2n\beta+\delta)) - j\,tanhb\, \cos(kr_1\gamma\sin(2n\beta+\delta))$$
$$-e^{a+j\mu d} \sin(kr_1\gamma\sin(2n\beta-\delta)) - j\,tanhb\, \cos(kr_1\gamma\sin(2n\beta-\delta))] \qquad (51)$$

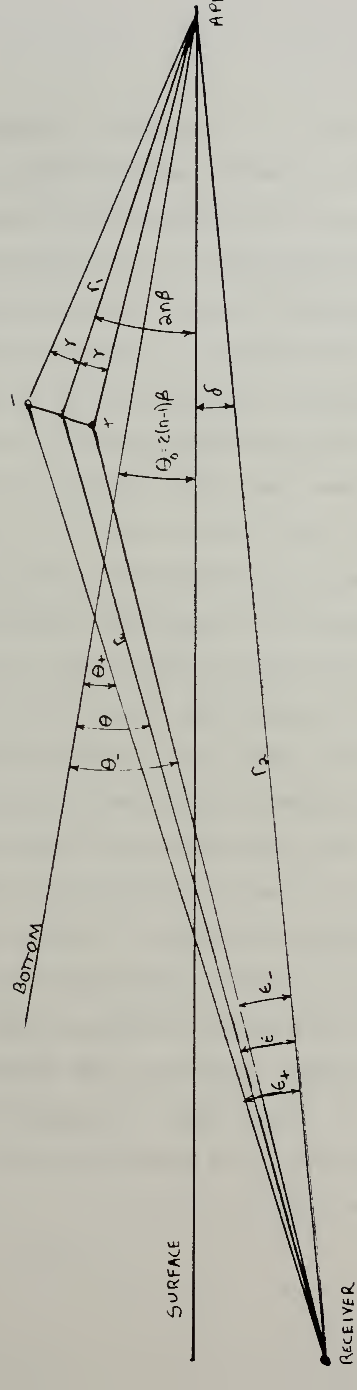
BOTTOM
SURFACE
RECEIVER
r_1
r_2
$2n\beta$
$\theta_0 = 2(n-1)\beta$
δ
γ
θ_+
θ
θ_-
ϵ_-
ϵ
ϵ_+

FIG. 3

VI. RESULTS

Three runs at different ranges were made to compare the output of the quadruplet model with that of the "URTEXT" program. For each run, the source angle is 1^0, and the wedge angle is 3^0. The ratio of the sound speed in seawater to that of the bottom is 1.01695, and the ratio of the density of seawater to that of the bottom is 0.7. This is equivalent to a slow bottom consisting of a combination of clay and ooze; conditions very common in continental shelf regions. The runs are tabulated at 0.30^0 increments of receiver angle from the surface downwards. The results are shown in tables 1 through 3. At a receiver angle of zero all three runs result in an amplitude of zero, as they should.

At the shortest range, Run 3, the results of the quadruplet model differ significantly from those of "URTEXT". The percentage difference in amplitude is consistently above 10%. With the exception of the 3^0 receiver angle, the average percentage difference in amplitude for the other two runs is well below 10%. The far field doublet approximation improves at longer ranges, and the approximations for Δr values become more accurate. Also, the difference in phase angle is much greater at the shortest range; half the phase angles in Run 3 differ by greater than $\pi/4$, but in the other two runs, only the phase angle at a 3^0 receiver angle differs by more than that amount.

Each of these data sets is accompanied by sample plots of the quadruplet pressure amplitude and the reflection coefficient for each quadruplet. In each case, the plots were taken with a receiver angle of 0.90^{0}. The magnitude of the complex quadruplet pressure drops off very quickly with the quadruplet number. It is negligible by the 5th quadruplet. This is a result of the effect of the rapid (exponential) decay of the Rayleigh reflection coefficient with increased angle of incidence of the higher number of quadruplet.

In practical terms, this means that the quadruplet expansion becomes less accurate with larger receiver and wedge angles. As these angles increase, the difference in the angles of incidence between the upper doublet sound path and the lower doublet sound path will increase proportionately. When these differences are raised to the exponential power in the reflection coefficients, the differences in amplitude between upper and lower doublets at the receiver will be quite large. However, the fundamental assumption in the quadruplet expansion is that the upper and lower doublet images are equivalent in amplitude, but opposite in phase. Therefore, the quadruplet expansion is only valid for very small angles and long ranges.

TABLE 1

BETA=3,GAMMA=1,R1=1,R2=100,DENSITY RATIO=.9,SPEED RATIO=1.01695

DELTA	URTEXT AMP.	QUAD AMP.	Δ% AMP.	URTEXT PHASE	QUAD PHASE	Δ^0 PHASE
0.30	0.00010	0.000092	8.4	17.6	-23.9	41.5
0.60	0.00018	0.000175	2.8	18.8	-23.3	42.1
0.90	0.00024	0.000243	1.25	19.2	-22.3	41.5
1.20	0.00032	0.000288	10.0	18.3	-20.8	39.1
1.50	0.00032	0.000306	4.4	17.5	-18.6	36.1
1.80	0.00030	0.000295	1.7	16.2	-15.4	31.6
2.10	0.00029	0.000255	12.0	16.0	-10.6	26.6
2.40	0.00020	0.000190	5.0	15.1	-2.1	17.2
2.70	0.00013	0.000112	13.9	18.2	19.4	1.2
3.00	0.00002	0.000079	295.0	26.9	88.5	61.6

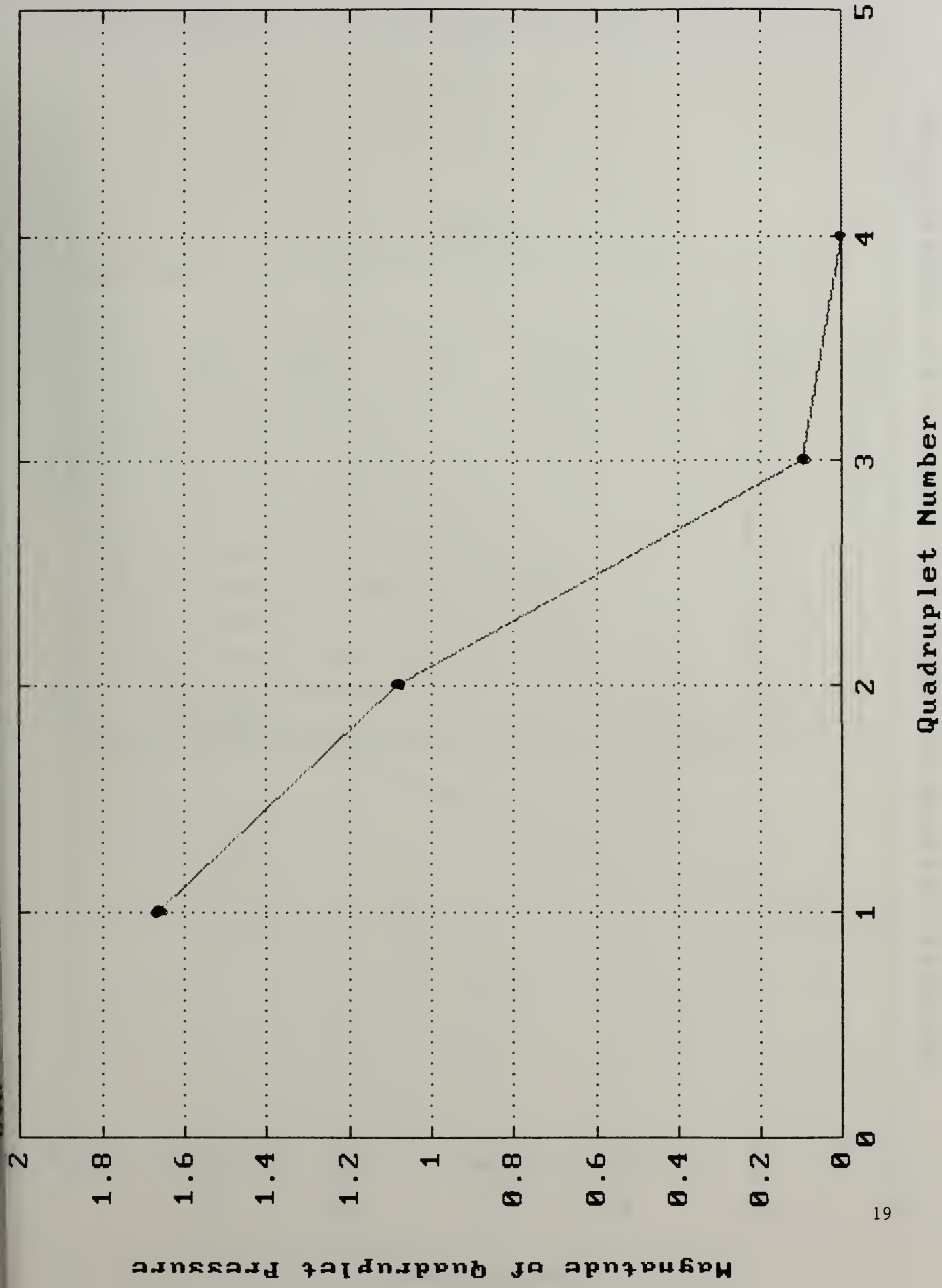
Quadruplet Number
Magnitude of Quadruplet Pressure

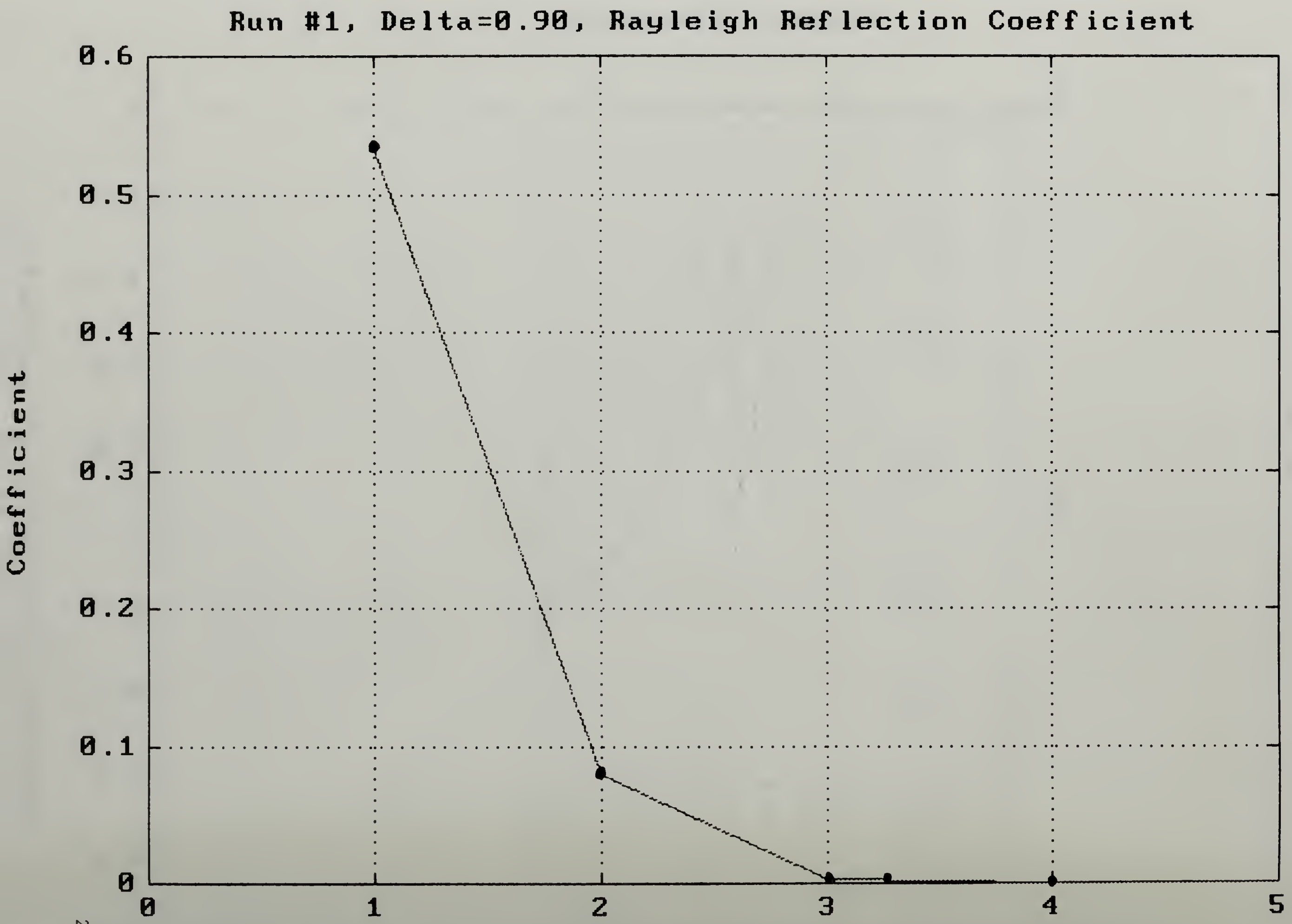

Run #1, Delta=0.90, Rayleigh Reflection Coefficient
Coefficient
0.6
0.5
0.4
0.3
0.2
0.1
0
0
1
2
3
4
5

TABLE 2

BETA=3,GAMMA=1,R1=1,R2=50,DENSITY RATIO=.9,SPEED RATIO=1.01695

DELTA	URTEXT AMP.	QUAD AMP.	Δ% AMP.	URTEXT PHASE	QUAD PHASE	Δ^0 PHASE
0.30	0.00018	0.000194	7.8	1.93	-22.9	24.8
0.60	0.00038	0.000369	2.9	2.75	-22.1	24.9
0.90	0.00052	0.000511	1.7	3.04	-20.7	23.7
1.20	0.00063	0.000606	3.8	3.95	-18.5	22.5
1.50	0.00065	0.000644	0.92	2.97	-15.3	18.3
1.80	0.00069	0.000620	10.1	4.72	-10.5	15.3
2.10	0.00059	0.000539	8.6	1.93	-2.71	4.64
2.40	0.00047	0.000416	11.5	2.59	11.5	8.9
2.70	0.00031	0.000303	2.3	4.85	42.3	37.5
3.00	0.00010	0.000321	221.0	18.1	-89.6	107.7

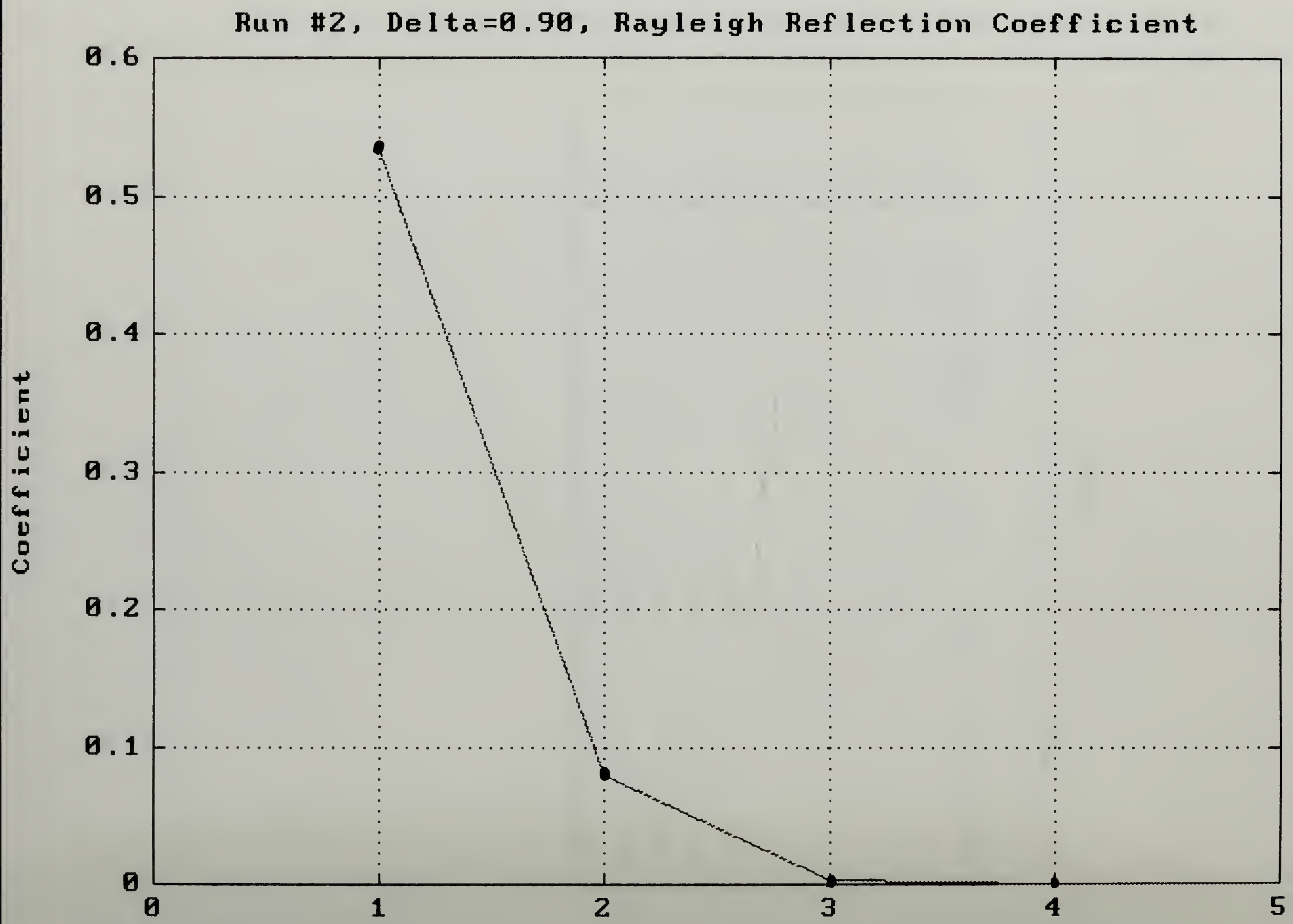

Run #2, Delta=0.90, Rayleigh Reflection Coefficient
Coefficient
0.6
0.5
0.4
0.3
0.2
0.1
0
0
1
2
3
4
5

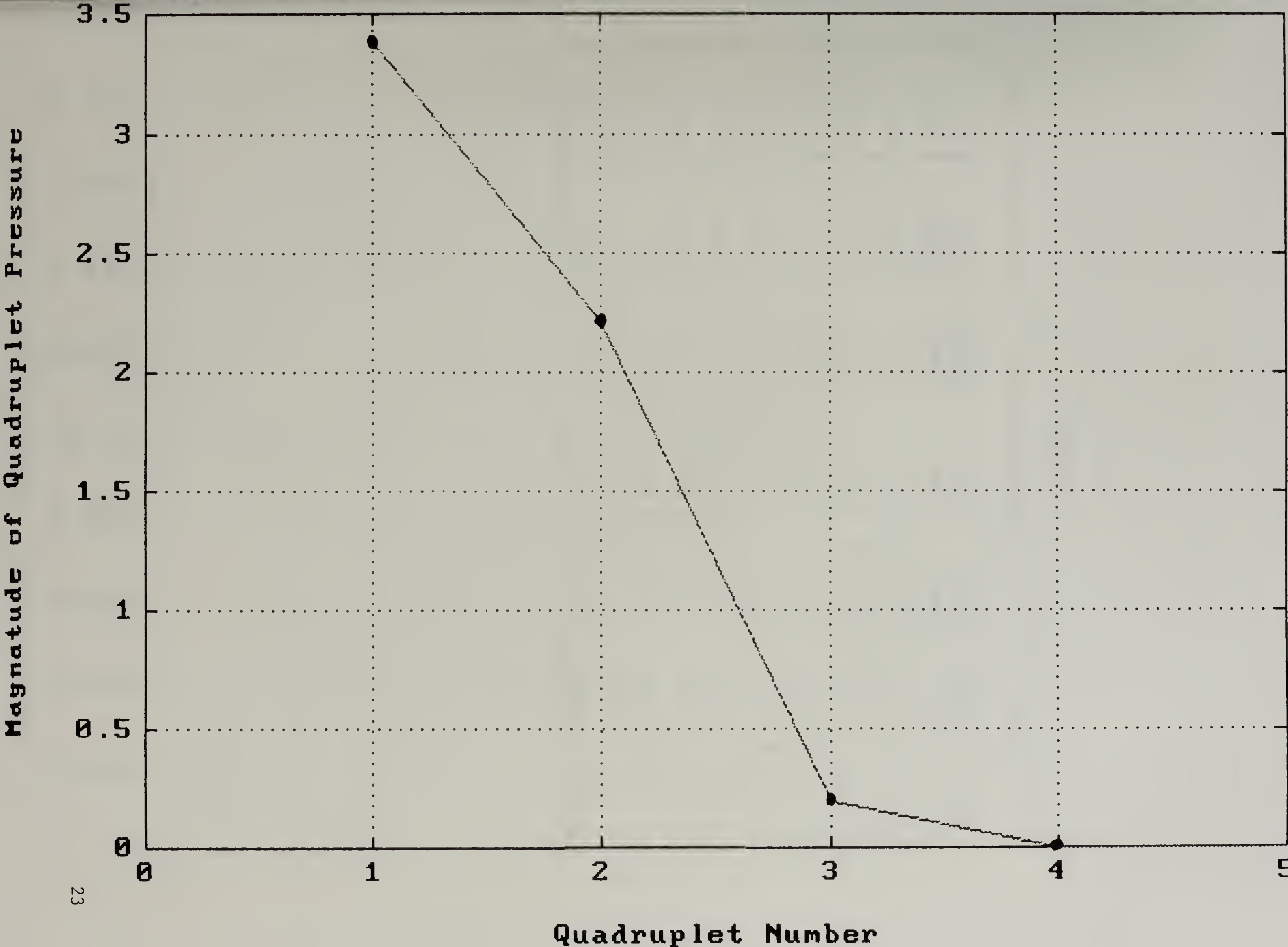

3.5
3
2.5
2
1.5
1
0.5
0
0
1
2
3
4
5
Magnatude of Quadruplet Pressure
Quadruplet Number

TABLE 3

BETA=3,GAMMA=1,R1=1,R2=10,DENSITY RATIO=.9,SPEED RATIO=1.01695

DELTA	URTEXT AMP.	QUAD AMP.	Δ% AMP.	URTEXT PHASE	QUAD PHASE	Δ^0 PHASE
0.30	0.0013	0.0015	15.4	-47.2	-27.5	19.7
0.60	0.0024	0.0028	16.7	-47.0	-25.4	21.6
0.90	0.0034	0.0039	14.7	-46.6	-21.4	25.2
1.20	0.0041	0.0046	12.2	-46.1	-15.1	31.0
1.50	0.0044	0.0050	13.6	-45.1	-5.58	39.5
1.80	0.0044	0.0051	15.9	-43.3	8.64	51.9
2.10	0.0040	0.0053	32.5	-40.2	28.33	68.5
2.40	0.0033	0.0061	84.8	-34.1	51.15	85.2
2.70	0.0024	0.0076	216.7	-20.1	71.85	92.0
3.00	0.0018	0.0098	444.4	13.5	87.68	74.2

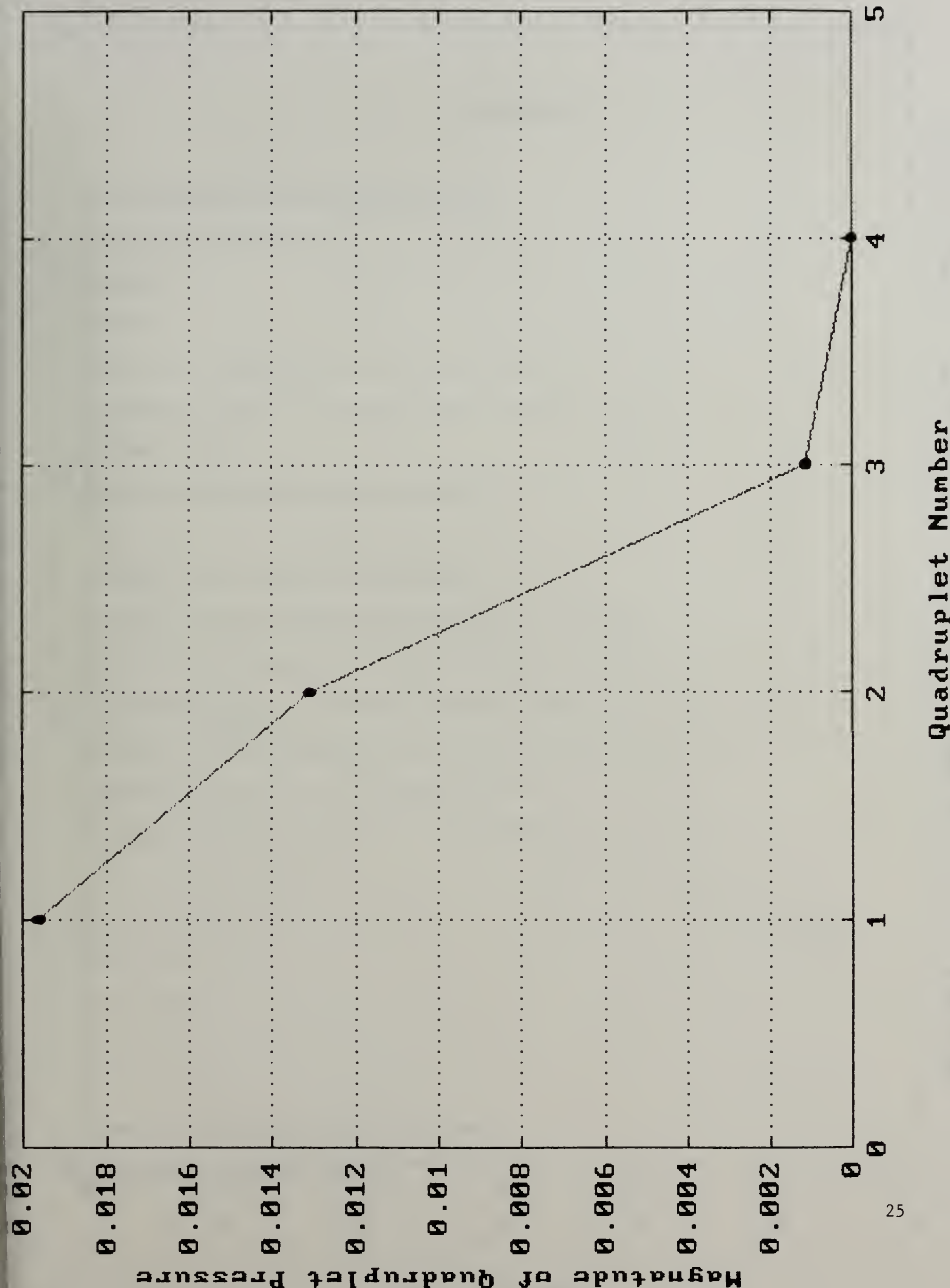
Magnitude of Quadruplet Pressure
Quadruplet Number
0
0.002
0.004
0.006
0.008
0.01
0.012
0.014
0.016
0.018
0.02
0
1
2
3
4
5

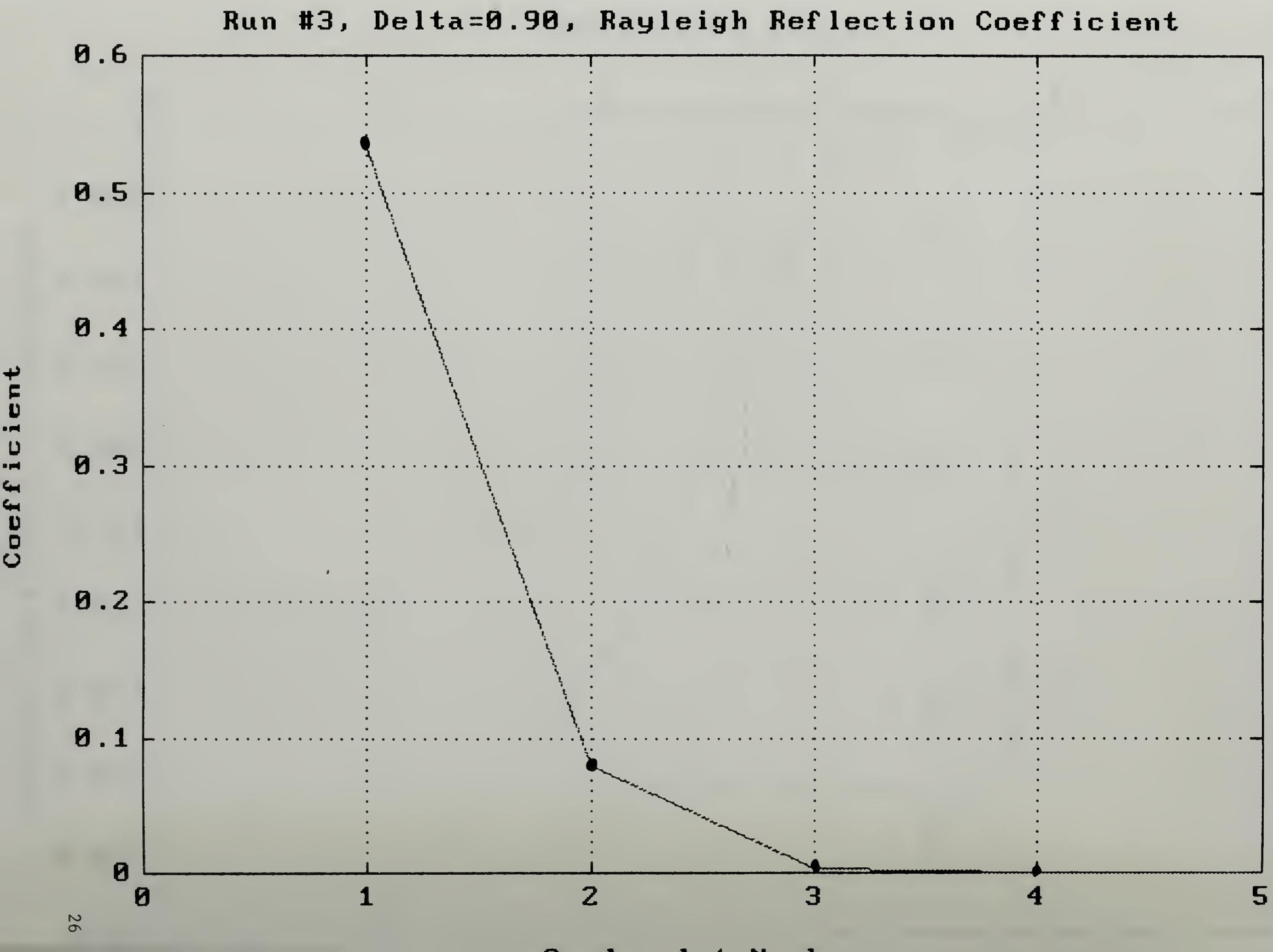
Run #3, Delta=0.90, Rayleigh Reflection Coefficient
Coefficient
0.6
0.5
0.4
0.3
0.2
0.1
0
0
1
2
3
4
5

APPENDIX A

```
%%%%%%%%%%%%%%%%%%%%%%%%%%%%%%%%%
%QUADRUPLET EXPANSION
%pquad.m
%MATLAB
%Quadruplet expansion of the acoustic
%pressure field in a wedge shaped ocean.
%Michael Joyce
%%%%%%%%%%%%%%%%%%%%%%%%%%%%%%%%%

B=input('wedge angle in degrees=');
G=input('source angle from surface in degrees=');
D=input('receiver angle from surface in degrees=');
rho=input('water to bottom density ratio=');
cc=input('water to bottom sound speed ratio=');
r1=input('range of source from apex=');
r2=input('range of receiver from apex=');

N1=fix(90/B);
B=B*pi/180;
G=G*pi/180;
D=D*pi/180;

%%%%%%%%%%%%%%%%%%%%%%%%%%%%%%%%%
%CALCULATE SCALING FACTOR
```

```
%%%%%%%%%%%%%%%%%%%%%%%%%%%%%%%%%%%%

tb=tan(B);
 if cc<1,
        t1=acos(cc);
        t2=sin(t1);
 else
        t1=acos(1/cc);
        t2=tan(t1);
 end
k1=2*t2*tb;
k=pi/k1;

%%%%%%%%%%%%%%%%%%%%%%%%%%%%%%%%%%%%
%CALCULATE CONSTANTS AND PRIMARY DOUBLET
%%%%%%%%%%%%%%%%%%%%%%%%%%%%%%%%%%%%

a1=2*(1/rho)/(sqrt(cc^2-1));
r=sqrt(r1^2+r2^2-2*r1*r2*cos(D));
r3=abs(r2-r1);
r4=r1*r2/r3^2;
mu=r2/abs(r2-r1);
q=k*r1*G*D;
p1=(2/r)*sin(q);
f=0;
```

```
%%%%%%%%%%%%%%%%%%%%%%%%%%%%%%%%
%QUADRUPLET SUMMATION
%%%%%%%%%%%%%%%%%%%%%%%%%%%%%%%%

 for n=1:1:N1,
        s(n)=n;
        th(n)=2*n*B;
        d(n)=k*r1*D*sin(th(n));
        phi(n)=k*r1*mu*(1-cos(th(n)));

        %%%%%%%%%%%%%%%%%%%%%%%%%
        %REFLECTION COEFFICIENTS
        %%%%%%%%%%%%%%%%%%%%%%%%%

        ru(n)=sqrt(r1^2+r2^2-2*r1*r2*cos(th(n)+D));
        rl(n)=sqrt(r1^2+r2^2-2*r1*r2*cos(th(n)-D));
        r5(n)=r1/ru(n);
        r6(n)=r1/rl(n);
        a1(n)=1+r5(n)*cos(th(n));
        b1(n)=r6(n)*cos(th(n));
        rr(n)=-B*a1*(n^2);
        R(n)=-exp(rr(n));
        a(n)=n*a1*D*a1(n);
        b(n)=n*a1*G*b1(n);

        %%%%%%%%%%%%%%%%%%%%%%%%%
```

```
%PRESSURE
%%%%%%%%%%%%%%%%%%%%%%%%%

ul(n)=cosh(b(n));
u2(n)=exp(-j*phi(n));
u3(n)=(-2/r)*R(n)*ul(n)*u2(n);

%%%%%%%%%%%%%%%%%%%%%%%%%
%UPPER IMAGE
%%%%%%%%%%%%%%%%%%%%%%%%%

v1(n)=sin(th(n)+D);
v2(n)=k*r1*G*v1(n);
v3(n)=sin(v2(n));
v4(n)=cos(v2(n));
v5(n)=-a(n)-j*mu*d(n);
v6(n)=exp(v5(n));
v7(n)=tanh(b(n));
v8(n)=v6(n)*(v3(n)-j*v7(n)*v4(n));

%%%%%%%%%%%%%%%%%%%%%%%%%
%LOWER IMAGE
%%%%%%%%%%%%%%%%%%%%%%%%%

w1(n)=sin(th(n)-D);
w2(n)=k*r1*G*w1(n);
```

```
        w3(n)=sin(w2(n));

        w4(n)=cos(w2(n));

        w5(n)=a(n)+j*mu*d(n);

        w6(n)=exp(w5(n));

        w7(n)=w6(n)*(w3(n)-j*v7(n)*w4(n));


        %%%%%%%%%%%%%%%%%%%%%%%%%

        %SUMMATION

        %%%%%%%%%%%%%%%%%%%%%%%%%


        p(n)=u3(n)*(v8(n)-w7(n));

        t=t+p(n);

        pr(n)=real(p(n));

        pim(n)=imag(p(n));

        pz(n)=sqrt(pr(n) 2+pim(n) 2);

        rm(n)=-1*R(n);

  end

plot(s,pz);grid;

xlabel('Quadruplet Number');

ylabel('Magnatude of Quadruplet Pressure');

title('Quadruplet Pressure');

pause;

plot(s,rm);grid;

title('Rayleigh Reflection Coefficient');

xlabel('Quadruplet Number');

ylabel('Coefficient');
```

```
pause;

ps=pl+f;

ph=imag(ps)/real(ps);

phl=atan(ph);

phase=180*phl/pi

f=f;

pl=pl;

ps=ps;

P=sqrt(real(ps) 2+imag(ps) 2)

end;
```

BIBLIOGRAPHY

Baek, C.; *The Acoustic Pressure in a Wedge Shaped Water Layer Overlying a Fast Fluid Bottom;* Master's Thesis, Naval Postgraduate School, Monterey, CA, March 1984

Bradshaw, N.; *Propagation of Sound in a Fast Bottom Underlying a Wedge Shaped Medium;* Master's Thesis, Naval Postgraduate School, Monterey, CA, Sept. 1980

Buckingham, M.J.; "The Theory of Three-dimensional Acoustic Propagation in a Wedgelike Ocean with a Penetrable Bottom;" *J. Acoust. Soc. Am.*, 82(1), July 1987

Coppens, A.B., Humphries, M., Sanders, J.V.; "Propagation of Sound out of a Fluid Wedge into an Underlying Fluid Substrate of Greater Sound Speed;" *J. Acoustic. Soc. Am.*, 76(5), November 1984

Coppens, A.B., Frey, A.R., Kinsler, L.E., Sanders, J.V.; *Fundamentals of Acoustics, Third Edition;* John Wiley, and Sons, Inc.; Monterey, CA, 1980

Coppens, A.B., Sanders, J.V., Ioannou, G.I., Kamawamura, M.; *Two Computer Programs for the Evaluation of the Acoustic Pressure Amplitude at the Bottom of a Wedge Shaped Fluid Layer Overlying a Fast, Fluid Half-Space;* Technical Report #NPS-61-79-002, Naval Postgraduate School, Monterey, CA, Dec. 1978

Jensen, F.B., Kuperman, W.A.; "Sound Propagation in a Wedge Shaped Ocean with a Penetrable Bottom;" *J. Acoustic. Soc. Am.*, 67(5), May 1980

Jensen, F.B., Tindle, C.T.; "Numerical Modeling Results for Mode Propagation in a Wedge;" *J. Acoustic. Soc. Am.*, 82(1), July 1987

Kaswandi, C.; *A Computerized Investigation Using the Method of Images to Predict the Sound Field in a Fluid Wedge Overlying a Slow Half-space;* Master's Thesis, Naval Postgraduate School, Monterey, CA, Dec. 1987

Kim Jong Rok; *Comparison for Sound Pressure in a Wedge Shaped Ocean as Predicted by an Image Method and a PE Model;* Master's Thesis, Naval Postgraduate School, Monterey, CA, Dec.1990

Livingood, D.M.; *Extension of the Analytical Approximation to the Transmission of Sound in Shallow Water Using the Image Model;* Master's Thesis, Naval Postgraduate School, Monterey, CA, Sept. 1992

Math Works, Inc.; *The Student Edition of MATLAB;* Prentice Hall, Inc., Englewood Cliffs, New Jersey, 07362

Nassopoulis, G.; *Study of Sound Propagation in a Wedge Shaped Ocean and Comparison with other Methods;* Master's Thesis, Naval Poastgraduate School, Monterey, CA, June 1992

Paliatsos, D.; *Computer Studies of Sound Propagation in a Wedge Shaped Ocean with Penetrable Bottom;* Master's Thesis, Naval Postgraduate School, Monterey, CA, March 1989

Personal Communications with A.B. Coppens and J.V. Sanders Naval Postgraduate School, Monterey, CA, June-Sept. 1993

DISTRIBUTION LIST

1. Defense Technical Information Center — 2
   Cameron Station
   Alexandria, VA, 22304-6145

2. Library, Code 0142 — 2
   Naval Postgraduate School
   Monterey, CA, 93943-5002

3. Dr. A.B. Coppens, Code PH/CZ — 2
   Department of Physics
   Naval Postgraduate School
   Monterey, CA, 93943-5002

4. Lt Michael D. Joyce — 2
   ASWOC Sigonella
   PSC 812, BOX 3270
   FPO AE 09627-3270

622-2